Scattering Function of Shallow Water Channels

H. Lew

DSTO-TR-0644

Scattering Function of Shallow Water Channels

H. Lew

Maritime Operations Division
Aeronautical and Maritime Research Laboratory

DSTO–TR–0644

ABSTRACT

The time and frequency spreading of a shallow water acoustic channel can be characterized by its scattering function. In order to exploit some of the time delay regularities in the acoustic channel, the scattering function is calculated using a Pekeris waveguide model. The correlator loss, which is a measure of the amount of signal spreading caused by the channel, is calculated as a function of range and depth for three well known classes of signals used in active sonar.

APPROVED FOR PUBLIC RELEASE

DEPARTMENT OF DEFENCE
DEFENCE SCIENCE & TECHNOLOGY ORGANISATION **DSTO**

Scattering Function of Shallow Water Channels

EXECUTIVE SUMMARY

Quieter submarines, as a result of improved noise and signature reduction, operating in littoral environments pose a challenging ASW detection problem for active sonar. Regardless of the quality of the sensors used and the skill of the sonar operators, the environment will still impose limitations on the sonar system's detection ability. One immediate problem is the lack of detailed knowledge of the environment (as well as the target and other operational factors) that can be used to develop suitable new algorithms. However, even if this knowledge were available, the amount of processing required would be unlikely to be cost effective.

Accepting that the complexity of the ocean environment can limit the level of acoustical information that can be sensed and usefully exploited, it is then reasonable, at least as a first step, to model the undersea acoustic channel as a random time-varying linear filter. For example, the scattering function, which is a measure of the second order statistics of the random time-varying filter, can be used to quantify the channel and hence ultimately sonar system performance.

In this paper the time and frequency spreading of a shallow water acoustic channel is characterized by its scattering function. In particular, its time spreading structure is calculated by using the Pekeris waveguide model. The Pekeris waveguide with a uniform sound speed profile is an attractive model from the viewpoint that only a minimal number of parameters are needed, but is sufficiently complex to exhibit many of the salient features observed in actual waveguides, at least to first order. By using such a model it is shown that signals with large time-bandwidth products are severely distorted by time and frequency dispersive channels. Although large time-bandwidth product signals are generally desirable for detection, clutter reduction and range resolution, it is clear that when operating in a dispersive channel these signals are of limited value when processed using conventional techniques such as simple matched filtering.

iv

Authors

H.Lew
Maritime Operations Division

Henry Lew completed B.E. (Electrical/Electronics) and B.Sc.(Hons-physics) degrees at the University of Melbourne in 1985 and 1986 respectively. He was awarded a Ph.D in physics at the University of Melbourne in 1990. From 1990 to 1995 he was a post-doctoral research fellow, working in the area of high energy physics, at the University of Melbourne, Purdue University and the Institute of Physics - Academia Sinica. In 1995 he joined DSTO as a research scientist working in the area of active sonar signal processing.

Contents

1 Introduction

Shallow water provides a challenge for designers of active sonar systems due to its fading multipath structure. The time and frequency spreading caused by the channel can adversely distort the transmitted signal and hence result in a degradation in sonar performance. In this paper, the limits of coherent pocessing (in the form of replica correlation or its matched filter equivalent), due to pulse distortion caused by the underwater medium, will be investigated. A simple and reasonably adequate model of an undersea acoustic channel is that of a random linear time-varying filter[1, 2, 3, 4]. The random nature is due to a lack of detailed knowledge of the acoustic environment (sound speed profile, bottom properties, surface motion etc) and the associated system parameters such as the geometry of the transmitter, receiver and target. Therefore, one is dealing with a complex dynamical system which warrants a stochastic description. For example, the scattering function which is a measure of the second order statistics of the random time-varying filter will be used to quantify the channel. This, however, is not to suggest that deterministic methods, such as wave equation solutions, are not useful. In this paper it is assumed that any regularities, as observed in an averaged sense, can be described by the deterministic wave equation. In particular, the Pekeris model will be used to account for the time delay structure of the scattering function.

The remainder of this paper is organized as follows: Section 2 provides the background for the scattering function description of the channel. Although the theory can be applied to the sonar detection and estimation problem in general, this paper will concentrate on one way transmission so that complications from target scattering need not be introduced. Section 3 gives details of the Pekeris waveguide. Section 4 applies the results of the previous sections to (a) a fully analytical case and (b) numerical cases for three classes of well known active sonar transmissions. Finally, section 5 concludes the paper.

2 Scattering function

Consider an active sonar system in which the transmitter and receiver are in separate locations. Let the transmitted signal be given by $s(t)$. By modelling the channel as a time-varying linear filter, the received signal $r(t)$ can be written as

$$r(t) = \int h(\tau, t) s(t - \tau) d\tau + n(t), \qquad (1)$$

where $h(\tau, t)$ is the channel impulse response at time t for a given delay τ and $n(t)$ is a noise term representing sea and thermal noise. For the purposes of this paper the ambient noise will not be discussed any further. The random impulse response $h(\tau, t)$ can considered as a member of an ensemble which describes the multipath and Doppler spread of the channel, where τ, for a fixed t, is a measure of the time delay spread a signal undergoes, and for a fixed τ, t indicates how rapidly the channel is changing with time, i.e., the amount of Doppler spreading. Usually, the channel response is characterized principally by its first and second moments, although higher order moments have been considered. The

first moment is taken to be zero due to the uncertainty in the phase, leaving the second moment, i.e., the covariance function, to carry the bulk of the statistical information about the channel.

In order to proceed further in the simplest way, two common assumptions are made. The first is that the channel response is a stationary random process for a given delay (range) interval[1]. This implies that the covariance function depends only on the time difference between measurements of the channel response. The second assumes that reflection or scattering of the channel is uncorrelated as a function of delay (range). These two assumptions then enable the covariance function to be written as

$$E\left\{h\left(\tau_1, t_1\right), h^*\left(\tau_2, t_2\right)\right\} = K\left(\tau_1, \Delta t\right) \delta\left(\tau_1 - \tau_2\right), \tag{2}$$

where $E\{\ \}$ denotes ensemble average, $\Delta t = t_1 - t_2$, and $K\left(\tau, \Delta t\right)$ is a two variable function dependent on the properties of the channel. From this two variable function it is useful to define the scattering function, $\sigma\left(\tau, f\right)$, such that

$$K\left(\tau, \Delta t\right) = \int_{-\infty}^{\infty} \sigma\left(\tau, f\right) e^{j2\pi f \Delta t} df. \tag{3}$$

Now assume that the receiver processes the received signal using a matched filter or correlator of the form

$$y\left(\tau, \phi\right) = \int r\left(t\right) s^*\left(t - \tau\right) e^{-j2\pi\phi t} dt, \tag{4}$$

where τ and ϕ are the relative delay and Doppler of the matched filter respectively. By using Eqs. (1) and (2) in (4), the mean power output of this matched filter is

$$E\left\{\left|y\left(\tau, \phi\right)\right|^2\right\} = \int \int \sigma\left(\lambda, f\right) \left|\chi\left(\lambda - \tau, f - \phi\right)\right|^2 df d\lambda, \tag{5}$$

where

$$\chi\left(\tau, \phi\right) = \int s\left(t\right) s^*\left(t - \tau\right) e^{-j2\pi\phi t} dt \tag{6}$$

is the ambiguity function of the pulse $s\left(t\right)$ and may be interpreted as the output of the matched filter for a received signal propagating through an ideal distortionless medium. Then the scattering function can be thought of as a two dimensional filter modifying the ideal channel matched filter response. Note that the ideal channel (i.e., a single path with no frequency spreading) is represented by $\sigma\left(\tau, f\right) = \delta\left(\tau\right) \delta\left(f\right)$.

Consider a time varying multipath channel described by its scattering function. A measure of how much the channel spreads the transmitted pulse can quantified by the correlator loss, defined as

$$CL = 10\log_{10}\left(F\right), \tag{7}$$

where the loss function, F, is given by

$$F = \frac{E\left\{\left|y\left(0, 0\right)\right|^2\right\}}{\left|\chi\left(0, 0\right)\right|^2}. \tag{8}$$

---

[1]This is equivalent to saying that the channel response is uncorrelated as a function of Doppler shift.

This is simply comparing the mean response of a time varying multipath channel to the ideal channel. It is convenient to normalize the scattering function by the quantity

$$\int \int \sigma\left(\lambda, f\right) df d\lambda \tag{9}$$

and also normalize the waveform, $s(t)$, to have unit energy so that $\chi(0,0) = 1$. The loss function then becomes

$$F = \frac{\int \int \sigma\left(\lambda, f\right) \left|\chi\left(\lambda, f\right)\right|^2 df d\lambda}{\int \int \sigma\left(\lambda, f\right) df d\lambda}. \tag{10}$$

Since the scattering function can be determined for any range and depth of interest, the normalization ensures the loss function is independent of the absolute signal level at any given position.

The main purpose of the loss function is to give an indication of how the energy of the transmitted signal is distributed by the channel. For example, values of the loss function close to one indicate the existence of a dominant path, while values much less than one suggest a number of different possibilites. It could be that the channel supports multiple paths or the channel distorts the signal by other means (e.g., frequency spreading) or a combination of both. The loss function by itself does not give enough information to distinguish between these possibilities.

It is clear that having some knowledge of the scattering function is essential in understanding and perhaps exploiting the effects of the environment on active sonar transmissions. To this end, assume that the scattering function can be written as

$$\sigma\left(\tau, \phi\right) = P\left(\tau\right) S_D\left(\phi\right), \tag{11}$$

where $P(\tau)$ is the delay power profile and $S_D(\phi)$ is the Doppler spread profile. Furthermore, the delay power profile is assumed calculable from the solutions of the wave equation subject to appropriate boundary condtions whereas the Doppler profile, without any apriori knowledge, is assumed to take the form

$$S_D\left(\phi\right) = \frac{1}{\sqrt{2\pi B_D^2}} \exp\left[-\frac{1}{2}\left(\frac{\phi}{B_D}\right)^2\right], \tag{12}$$

where B_D is the variance of the Doppler spread. Note that the assumed separability of the scattering function into the delay power profile and the Doppler spread profile implies that the mechanisms responsible for Doppler spreading are statistically independent of the range interval under observation. This assumption is also motivated by how one would go about measuring the scattering function without sophisticated signal processing. To see this, consider a time varying multipath channel. The delay power profile can be determined by probing the channel with a short pulse and measuring the average echo power as a function of delay. The Doppler profile can be measured by CW (continuous wave) testing of the channel to give the frequency spectrum of the average received power.

3   Pekeris waveguide

In this section the delay power profile will be calculated by using the Pekeris waveguide[5] to model the shallow water channel. The geometry of the channel is shown in Fig. 1. The

Pekeris model is chosen because it exhibits many of the characteristics of real waveguides without being overly complicated mathematically. The channel is completely specified by the depth of water, H, the sound speed profiles of the water and bottom, $c(z)$ and $c_b(z)$, the densities of the water and bottom, ρ and ρ_b, and a pressure release at the air-water interface. In fact closed form solutions can be found for special cases of interest[6]. The pressure time series as a function of range and depth for an arbitrary source waveform[7] can be expressed in terms of normal modes[2], i.e.,

$$p(t,r,z) = \int (-j\pi) \sum_m \psi_m(z_0)\psi_m(z) H_0^{(2)}(k_m r) S(f) e^{j2\pi ft} df, \qquad (13)$$

where $S(f)$ is the Fourier spectrum of the transmitted waveform, $s(t)$, $\psi_m(z)$ is the mth normal mode eigenfunction as a function of depth, $H_0^{(2)}$ is a Hankel function, and k_m is the horizontal wavenumber which is related to the sound speed profile, $c(z)$, the source frequency, f, and vertical wavenumber, γ_m, by

$$k_m^2(z) + \gamma_m^2 = \left(\frac{2\pi f}{c(z)}\right)^2. \qquad (14)$$

In order to probe the channel's multipath structure, a very broadband source should be used. In doing so, the delay power profile can be estimated from Eq.(13) as

$$P(\tau) = \left| \int \sum_m \sqrt{\frac{2\pi}{k_m r}} \psi_m(z_0)\psi_m(z) e^{j[2\pi f(\tau+t_0) - k_m r - \pi/4]} df \right|^2 \qquad (15)$$

where the Hankel function has been replaced by the exponential in the long range approximation, t_0 is beginning of the observation time window (or is the time when $P(0)$ is maximum) and τ is time delay relative to t_0.

Two cases with uniform sound speed profiles will be considered: (i) rigid bottom and (ii) fluid bottom. The rigid bottom case can be solved exactly and the delay power profile is given by

$$P(\tau) = \sum_{m=0}^{\infty} \sum_{i=1}^{4} \frac{1}{(c\tau_{im})^2} \delta(\tau + t_0 - \tau_{im}), \qquad (16)$$

where

$$c\tau_{1m} = \sqrt{r^2 + (z - z_0 + 2mH)^2}$$

$$c\tau_{2m} = \sqrt{r^2 + (z + z_0 + 2mH)^2}$$

$$c\tau_{3m} = \sqrt{r^2 + (z + z_0 - 2(m+1)H)^2}$$

$$c\tau_{4m} = \sqrt{r^2 + (z - z_0 - 2(m+1)H)^2}. \qquad (17)$$

The derivation of this result is given in the Appendix.

---

[2]Note that representations of solutions to the wave equation other than normal modes can be used. It turns out the normal mode method is especially convenient for calculating the sound field as a function of range and depth.

For the fluid bottom case the delay power profile is calculated by evaluating Eq.(15) numerically because there is no simple analytic solution available. The modal eigenfunctions for the water column are given by

$$\psi_m(z) = A_m \sin(\gamma_m z), \tag{18}$$

where

$$A_m^2 = 2\gamma_m \left[\gamma_m H - \cos(\gamma_m H) \sin(\gamma_m H) - b^2 \sin^2(\gamma_m H) \tan(\gamma_m H)\right]^{-1} \tag{19}$$

is a normalization constant[3] and $b = \rho/\rho_b$. The corresponding eigenvalues are obtained by solving

$$\tan(\gamma_m H) = -\frac{\gamma_m H}{b\sqrt{a^2 - \gamma_m^2 H^2}}, \tag{20}$$

where

$$a = 2\pi f H \sqrt{\frac{1}{c^2} - \frac{1}{c_b^2}}. \tag{21}$$

Note that the existence of analytic solutions is valuable in that they reveal physical insight to the problem and provide a check, in limiting cases, on numerical solutions to problems where exact solutions are either impossible or extremely difficult to obtain. This is the role of the rigid bottom case and it is clear that in going from the rigid bottom case to the fluid bottom case the computational difficulties have greatly increased.

4 Applications

4.1 Analytic example

Consider a Gaussian LFM signal transmitted through an ideal rigid bottom shallow water channel. A complete analytical expression of the loss function is available in this case. Let the transmitted signal have a Gaussian envelope of the form

$$s(t) = \left(\frac{2}{\pi T^2}\right)^{\frac{1}{4}} \exp\left[-\left(\frac{t}{T}\right)^2\right] \exp\left[j\pi W \frac{t^2}{T}\right], \tag{22}$$

where T is the effective duration of the pulse and W is frequency sweep width (the CW case is obtained by setting $W = 0$). By using Eq.(6), the ambiguity function is[4],

$$|\chi(\tau, \phi)|^2 = \exp\left[-\left(\frac{\tau}{T}\right)^2\right] \exp\left[-\pi^2 (\phi T - W\tau)^2\right]. \tag{23}$$

---

[3]The wave solutions of the depth dependent part of the Helmholtz equation form an orthonormal set. The normalization constant is obtained by having these solutions satisfy the boundary and orthogonality conditions.

The loss function of Eq.(10) for the rigid bottom channel (via Eqs. (11), (12) and (16)) is

$$F = \frac{1}{N\sqrt{2\pi B_D^2}} \sum_{m=0}^{\infty} \sum_{i=1}^{4} \frac{1}{(c\tau_{im})^2} \int_{-\infty}^{\infty} |\chi(\Delta\tau_{im}, \phi)|^2 \exp\left[-\frac{1}{2}\left(\frac{\phi}{B_D}\right)^2\right] d\phi, \quad (24)$$

where $\Delta\tau_{im} = \tau_{im} - t_0$ is the excess delay and the normalization factor is given by

$$N = \sum_{m=0}^{\infty} \sum_{i=1}^{4} \frac{1}{(c\tau_{im})^2}. \quad (25)$$

For the Gaussian pulse, the loss function becomes

$$F = \frac{1}{N\sqrt{1 + 2\pi^2 B_D^2 T^2}} \sum_{m=0}^{\infty} \sum_{i=1}^{4} \frac{1}{(c\tau_{im})^2} \exp\left[-\frac{\Delta\tau_{im}^2}{T^2}\right] \exp\left[-\frac{\pi^2 W^2 \Delta\tau_{im}^2}{(1 + 2\pi^2 B_D^2 T^2)}\right]. \quad (26)$$

This example explicitly shows how a signal cannot be transmitted with an arbitrarily large pulse duration and/or bandwidth in a dispersive channel without incurring significant signal spreading. More specifically, $F \ll 1$ if

$$T \gg T_c \equiv \frac{1}{\sqrt{2\pi} B_D} \text{ and/or}$$

$$W \gg B_c \equiv \frac{1}{\pi \Delta\tau} \quad (27)$$

where $\Delta\tau$ is the average excess delay, and T_c and B_c denote the coherence time and coherence bandwidth respectively. Conversely, the dispersive effects of the channel can be considered unimportant if the sonar waveform's duration and bandwidth are operated within their coherence limits, though this might not be possible in practice. Note that these conclusions hold in general though the expressions for T_c and B_c will differ according to the channel and waveforms under consideration.

Figure 2 shows an example of the correlator loss as a function of range and depth assuming a source depth of 10 m and a rigid bottom of depth 100 m. Fig. 3(a) gives an example of the Gaussian LFM ambiguity function. It can be seen from Fig. 2 that the loss function decreases with range and is largely insensitive to changes in depth. When the source and receiver are relatively close to each other the direct path is dominant as the other paths have longer path lengths and are weaker in strength (recall that the amplitude of each path is inversely proportional to the path length). This means that the loss function should be near unity if, for the moment, Doppler spreading is neglected. As the range increases, the direct path becomes less dominant relative to the other paths and the spread of the delay power profile becomes larger, resulting in a smaller value for the loss function. At very long ranges, all the paths are nearly comparable as the path difference between paths falls off inversely with range (see Eq. (17)) and hence the loss function decreases slowly with range. This is analogous to the well known phenomenon of energy spreading in a shallow water channel, i.e., the transition from spherical to cylindrical spreading.

An order of magnitude estimate of the loss function or the correlator loss can be obtained by considering the following artificial, but instructive, example. Assume that the received signal from a multipath channel can be represented by a sum of time delayed replicas of the transmitted waveform and each path is roughly equivalent. Then the

received signal can written as $r(t) = 1/\sqrt{N} \sum_{k=1}^{N} \phi_k(t)$ where N is the number of paths and $\phi_k(t)$ is the kth delayed replica of the transmitted waveform. The correlator output for the received waveform has a series of peaks with amplitude $\sim 1/\sqrt{N}$. This gives a correlator loss of $CL \sim -10 \log_{10} N$. For example, 10 to 100 paths results in a correlator loss of -10 to -20 dB, in broad agreement with the results shown in Fig. 2. Also notice that the correlator loss for the LFM signal is worse than that of CW pulse. This is not unexpected since the larger bandwidth of the LFM signal allows it to resolve a greater number of paths.

4.2 Numerical examples

In this section the correlator loss as a function of range and depth will be calculated for both the rigid bottom and fluid bottom cases using three well known classes of sonar signals, as characterized by their ambiguity functions[3, 8]. They are the (i) ridge (e.g., rectangular CW pulse), (ii) sheared ridge (e.g., rectangular LFM pulse) and (iii) thumbtack (e.g., pseudo-random noise) ambiguity functions given respectively by

$$|\chi(\tau,\phi)|^2 = \left[\frac{T - |\tau|}{T} \frac{\sin \pi \phi (T - |\tau|)}{\pi \phi (T - |\tau|)}\right]^2, \ |\tau| \le T \qquad (28)$$

$$|\chi(\tau,\phi)|^2 = \left[\frac{T - |\tau|}{T} \frac{\sin \pi \zeta (T - |\tau|)}{\pi \zeta (T - |\tau|)}\right]^2, \ |\tau| \le T \qquad (29)$$

$$|\chi(\tau,\phi)|^2 = \left[\frac{T - |\tau|}{T} \frac{\sin \pi \tau W}{\pi \tau W} \frac{\sin \pi \phi (T - |\tau|)}{\pi \phi (T - |\tau|)}\right]^2$$
$$+ \frac{1}{TW}\left(1 - \frac{|\tau|}{T}\right)\left(1 - \frac{|\phi|}{W}\right) \ |\tau| \le T, \ |\phi| \le W, \qquad (30)$$

where $\zeta = \phi - W\tau/T$ and the last equation (representing the thumbtack ambiguity function) assumes $TW \gg 1$. The ambiguity functions are zero for $|\tau| \ge T$ and the last term of the thumbtack ambiguity function is zero when $|\phi| \ge W$. The delay-Doppler characteristics of these ambiguity functions are illustrated in Figs. 3(b), 3(c) and 3(d) respectively. The following parameter set will be used for the examples:

Pulse duration, $T = 0.5$ s

Frequency sweep width, $W = 0$ for CW and $W = 200$ Hz for others

Observation window length of 2 s

Centre frequency, $f_c = 1000$ Hz

Frequency window, 800 - 1200 Hz

Sampling frequency, $f_s = 4096$ Hz

Source depth, $z_0 = 10$ m

Channel depth, $H = 100$ m

Sound speed in water, $c = 1500$ m/s

Density of water, $\rho = 1000$ kg/m^3

Sound speed of "typical" bottom, $c_b = 1600$ m/s

Density of "typical" bottom, $\rho_b = 1500$ kg/m^3

Sound speed of low reflective bottom, $c_b = 1510$ m/s

Density of low reflective bottom, $\rho_b = 1010$ kg/m^3

Doppler spread, $B_D = 1$ Hz

Note that the Doppler spread[4] is calculated by assuming a range rate spreading of $v \sim 2$ knot which gives a Doppler shift of about 1.4 Hz. So $B_D = 1$ Hz is taken as the nominal value.

Closed form expressions of the loss function for the rigid bottom case using the ridge and thumbtack ambiguity functions can be calculated from Eqs.(28), (30) and (24). There is no simple form for the sheared ridge ambiguity function but a relatively simple upper bound can be obtained. Their expressions are given as follows: For the ridge ambiguity function,

$$F = \frac{1}{N\sqrt{2\pi}B_D T} \sum_{m=0}^{\infty} \sum_{i=1}^{4} \frac{1}{(c\tau_{im})^2} \, f\left(\Delta\tau_{im}\right) \, I, \tag{31}$$

while for sheared ridge

$$F < \frac{1}{N\sqrt{2\pi}B_D T} \sum_{m=0}^{\infty} \sum_{i=1}^{4} \frac{1}{(c\tau_{im})^2} \, f\left(\Delta\tau_{im}\right) \, \exp\left[-\frac{1}{2}\left(\frac{W\Delta\tau_{im}}{B_D T}\right)^2\right], \tag{32}$$

and for the thumbtack ambiguity function

$$F = \frac{1}{N\sqrt{2\pi}B_D T} \sum_{m=0}^{\infty} \sum_{i=1}^{4} \frac{1}{(c\tau_{im})^2} \, f\left(\Delta\tau_{im}\right) \left\{\frac{\sin^2\left(\pi W\Delta\tau_{im}\right)}{\left(\pi W\Delta\tau_{im}\right)^2} \, I + \frac{B_D}{W}J\right\}, \tag{33}$$

where

$$f\left(\tau\right) = \begin{cases} 1 - \frac{|\tau|}{T} & \text{if } |\tau| < T \\ 0 & \text{otherwise,} \end{cases} \tag{34}$$

$$\begin{aligned} I &= \text{erf}\left(\sqrt{2}\pi k B_D\right) - \frac{1}{\pi\sqrt{2\pi}k B_D}\left(1 - e^{-2\pi^2 k^2 B_D^2}\right) \\ J &= \sqrt{2\pi}\,\text{erf}\left(\frac{W}{B_D\sqrt{2}}\right) - \frac{2B_D}{W}\left(1 - e^{-\frac{W^2}{2B_D^2}}\right), \end{aligned} \tag{35}$$

$k = Tf\left(\Delta\tau_{im}\right)$ and erf($\cdot$) is the error function[5]. The loss functions of the three signal types are shown in Figs. 4, 5 and 6 as a function of range and depth.

---

[4]The Doppler shift is given by $\phi = 2f_c v/c \sim 0.7\left(\frac{f_c}{kHz}\right)\left(\frac{v}{knot}\right)$ Hz.

[5]The error function is defined as $\text{erf}(x) = \frac{2}{\sqrt{\pi}}\int_0^x \exp\left(-t^2\right) dt$.

Unfortunately, no closed form expressions are available for the fluid bottom case. As a result the scattering and loss functions are evaluated numerically for each target range and depth of interest. An example of the scattering function for a range of 10 km and a depth of 10 m is shown in Fig. 7. The correlator loss for the three signal types of a "typical" Pekeris waveguide is shown in Figs. 8 to 10. Figures 11 to 13 show the case when the waveguide has a less reflective bottom. It can be seen that the correlator loss, a quantitative measure of signal spreading, decreases in going from a fully reflective bottom to a less reflective one for all signal types. Note that the number of paths increases when approaching the rigid bottom limit. In such cases the transmitted signal suffers more distortion since more paths contribute to the interference. At the same time, the superposition of a large number of paths tends to have an averaging or smoothing effect on the correlator loss (see Eq.(10)) as a function of range and depth. Furthermore, the signal distortion increases with range since the number of significant paths for a given arrival point should also increase with range. Finally, since the channel under consideration is predominantly a delay spread one, signals with large time-bandwidth products, such as LFM and PRN, will suffer the most degradation[6] (see Eq.(27)).

5 Conclusions

The scattering function provides a useful statistical characterization of acoustic undersea channels in active sonar applications. In particular, the shallow water channel can be modelled by the Pekeris waveguide. The Pekeris waveguide with a uniform sound speed profile is an attractive model from the point of view of needing only few parameters but is otherwise sufficiently complex to exhibit many of the salient features observed in actual waveguides, at least to first order. By using such a model it was shown that signals with large time-bandwidth products are severely distorted by dispersive channels. Although large time-bandwidth product signals are generally desirable for detection, clutter reduction and range resolution, it is clear that when operating in a channel with time and frequency spreading these signals are of limited value when processed using conventional techniques such as simple matched filtering.

Acknowledgment

---

[6]Notice that for the two CW cases (fluid bottom) in Figs. 8 and 11, there appears a ridge in the correlator loss function for depths near the bottom of the channel. This is caused by the consistently nonzero value of the modal amplitudes near the bottom of the waveguide (see Figs. 5.3 and 5.15 of Ref.[6]). For broadband signals, the sum over a large number of frequency components is expected to wash out this effect. A similar argument applies for channels with highly reflective bottoms where the existence of a larger number of trapped propagating modes can also cause a cancellation.

6 Appendix

For an isospeed rigid bottom channel the modal eigenvalues and eigenfunctions in Eq.(13) are given by

$$\gamma_m = \left(m + \frac{1}{2}\right)\frac{\pi}{H} \text{ for } m = 0, 1, 2, \ldots \tag{36}$$

$$\psi_m(z) = \sqrt{\frac{2}{H}} \sin(\gamma_m z), \tag{37}$$

respectively. By using the following results

$$\gamma_m = -\gamma_{m-1} \tag{38}$$

$$\sum_{m=0}^{\infty} 2\sin(\gamma_m z_0)\sin(\gamma_m z) H_0^{(2)}(k_m r) = \sum_{m=-\infty}^{\infty} \sin(\gamma_m z_0)\sin(\gamma_m z) H_0^{(2)}(k_m r) \tag{39}$$

$$\int_{-\infty}^{\infty} H_0^{(2)}\left(r\sqrt{\left(\frac{2\pi f}{c}\right)^2 - \gamma^2}\right) e^{j2\pi ft} df = j\frac{c}{\pi}\frac{e^{-j\gamma\sqrt{c^2 t^2 - r^2}}}{\sqrt{c^2 t^2 - r^2}} \tag{40}$$

$$\int_{-\infty}^{\infty} S(f) e^{j2\pi ft} df = s(t) \tag{41}$$

Eq.(13) becomes

$$
\begin{aligned}
p(t, r, z) &= \frac{c}{H}\sum_{m=-\infty}^{\infty}\sin(\gamma_m z_0)\sin(\gamma_m z)\int_{-\infty}^{\infty} s(t - \tau)\frac{e^{-j\gamma_m\sqrt{c^2\tau^2 - r^2}}}{\sqrt{c^2\tau^2 - r^2}} d\tau \\
&= \frac{c}{4H}\int_{-\infty}^{\infty}\frac{s(t - \tau)}{\sqrt{c^2\tau^2 - r^2}}\sum_{m=-\infty}^{\infty}\left\{e^{j\gamma_m\xi_1} + e^{j\gamma_m\xi_2} - e^{j\gamma_m\xi_3} - e^{j\gamma_m\xi_4}\right\} d\tau,
\end{aligned}
\tag{42}
$$

where

$$
\begin{aligned}
\xi_1 &= z - z_0 - \sqrt{c^2\tau^2 - r^2} \\
\xi_2 &= -z + z_0 - \sqrt{c^2\tau^2 - r^2} \\
\xi_3 &= z + z_0 - \sqrt{c^2\tau^2 - r^2} \\
\xi_4 &= -z - z_0 - \sqrt{c^2\tau^2 - r^2}.
\end{aligned}
\tag{43}
$$

The above expression can be furthered simplified by using

$$\sum_{m=-\infty}^{\infty} e^{j2\pi m\frac{t}{T}} = \sum_{m=-\infty}^{\infty} T\,\delta(t - mT) \tag{44}$$

$$\delta[f(x_i)] = \sum_i \left|\frac{df}{dz}\right|_{x=x_i}^{-1} \delta(x - x_i), \text{ for } f(x_i) = 0. \tag{45}$$

The result, after some manipulation, is

$$p(t, r, z) = \sum_{m=-\infty}^{\infty}\left\{\frac{s(t - \tau_a)}{c\tau_a} - \frac{s(t - \tau_b)}{c\tau_b}\right\}, \tag{46}$$

where

$$
\begin{aligned}
c\tau_a &= \sqrt{r^2 + (z - z_0 + 2mH)^2} \\
c\tau_b &= \sqrt{r^2 + (z + z_0 + 2mH)^2}
\end{aligned}
\tag{47}
$$

or in the more commonly used form

$$
p(t, r, z) = \sum_{m=0}^{\infty} (-1)^m \sum_{i=1}^{4} \frac{(-1)^{i+1}}{(c\tau_{im})} \, s(t - \tau_{im}),
\tag{48}
$$

where τ_{im} are given by Eq.(17). The result of Eq.(16) easily follows from this by using $s(t) = \delta(t)$.

References

1. E. C. Westerfield, R. H. Prager and J. L. Stewart, "Processing gains against reverberation (clutter) using matched filters", IRE Trans. Information Theory, **IT-6**, 342 (1960).

2. A. W. Ellinthorpe and A. H. Nuttall, "Theoretical and empirical results on the characterization of undersea acoustic channels", Ist IEEE Ann. Communications Conf., p. 585 (1965).

3. J. P. Costas, "Medium constraints on sonar design and performance", EASCON '75 Convention Record, 68-A (1975).

4. H. L. Van Trees, "Detection, estimation and modulation", **Part III**, Wiley (1971).

5. C. L. Pekeris, "Theory of propagation of explosive sound in shallow water" in Propagation of Sound in the Ocean, Geol. Soc. Amer., Mem. 27, 1948.

6. G. V. Frisk, "Ocean and seabed acoustics: A theory of wave propagation", Prentice Hall (1994).

7. L. M. Brekhovskikh, "Waves in layered media", 2nd Ed., Academic Press (1980).

8. T. H. Glisson, C. I. Black and A. P. Sage, "On sonar signal analysis", IEEE Trans. Aerospace and Electronic Systems, **AES-6**, 37 (1970).

Figure 1: Geometry of the Pekeris waveguide.

Figure 2: Correlator loss of (a) a Gaussian CW pulse and (b) its corresponding contour plot. Similarly for (c) and (d) but for a Gaussian LFM pulse. The shallow water channel is isospeed with a rigid bottom.
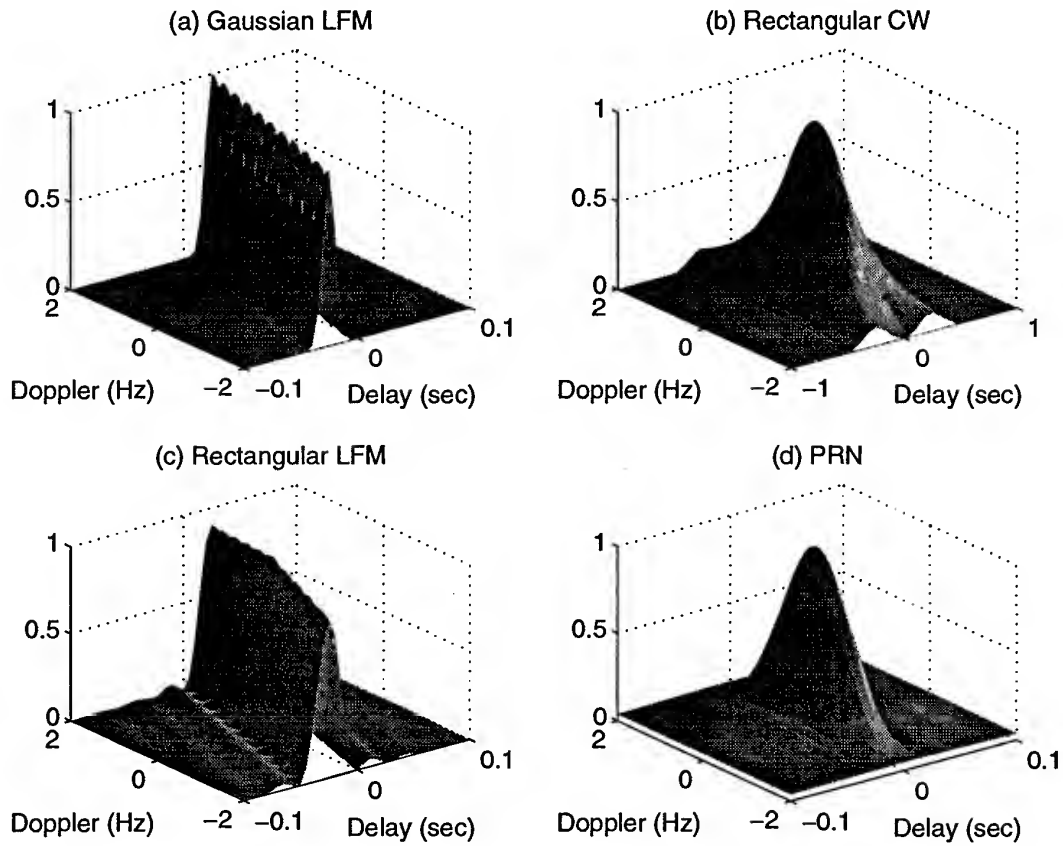
Figure 3: Ambiguity functions for (a) Gaussian LFM, (b) rectangular CW, (c) rectangular LFM, and (d) PRN (pseudo-random noise). These are shown using $T = 0.5$ s and $W = 40$ Hz ($W = 0$ for CW) in order to accentuate their features.
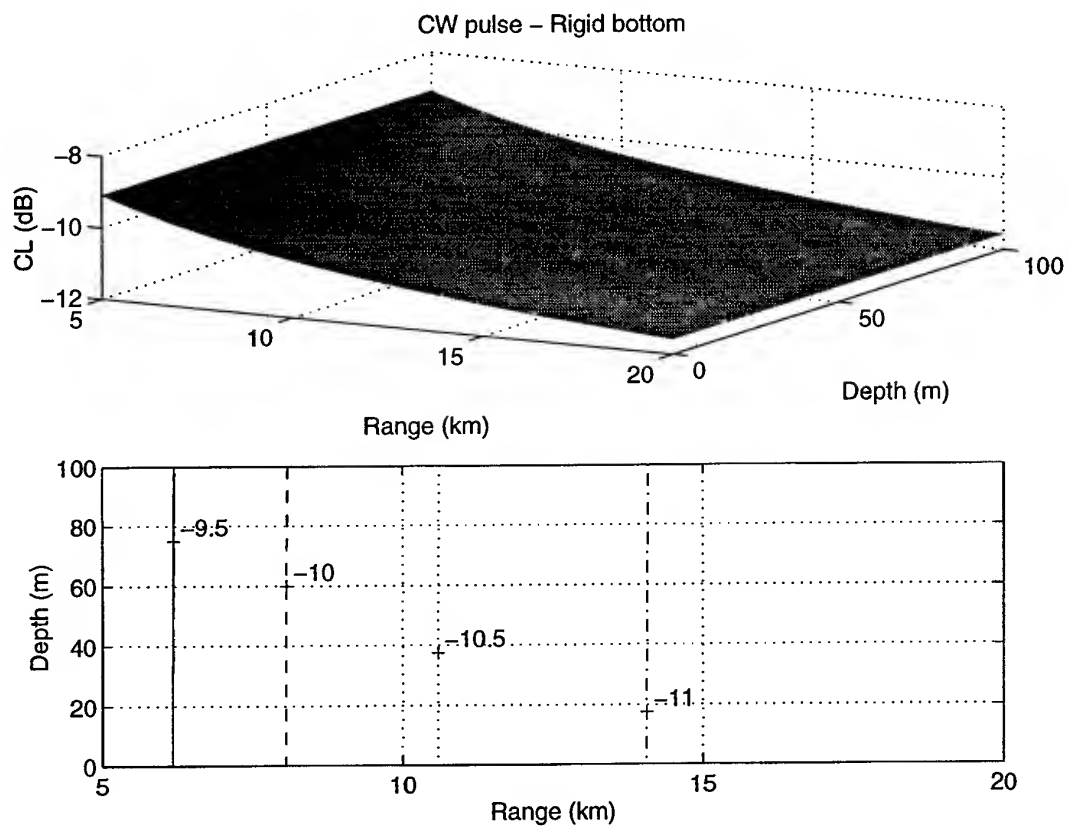
CW pulse – Rigid bottom

Figure 4: The correlator loss of a CW pulse (T = 0.5 s) in an isospeed channel with a
rigid bottom. The contour plot shows four levels: CL = −9.5 dB (solid), −10 dB (dashed),
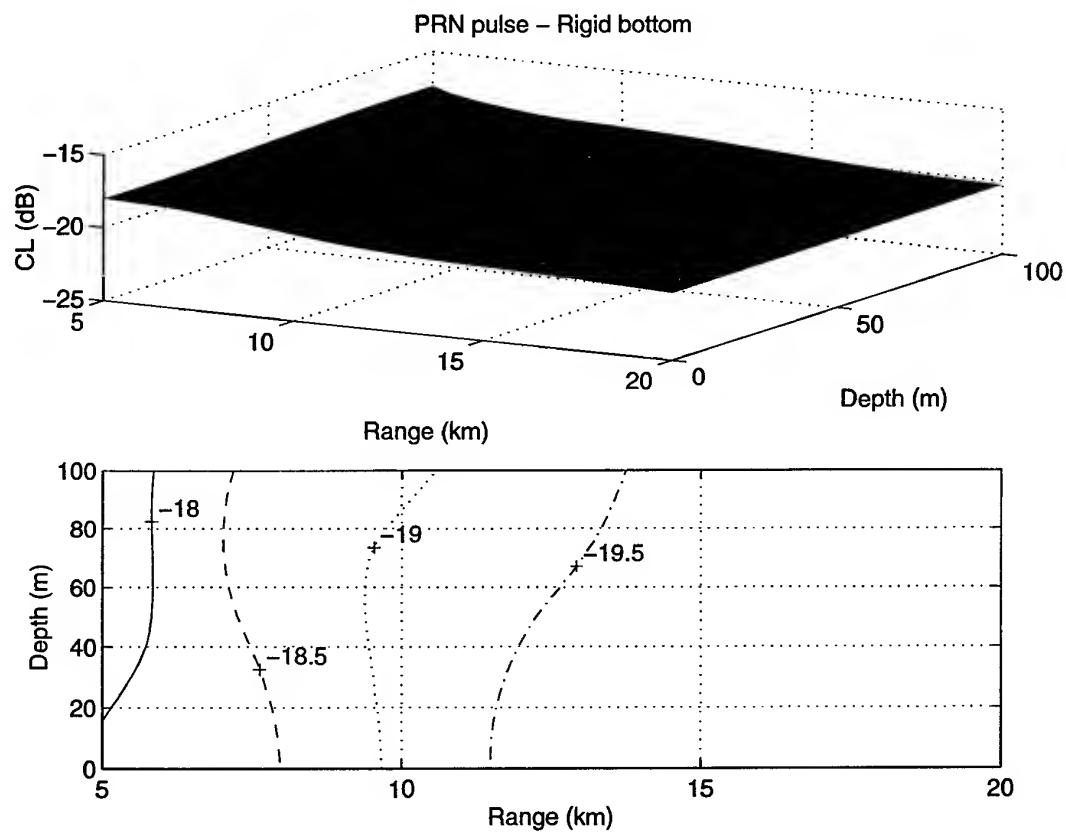−10.5 dB (dotted) and −11 dB (dashdot).

Figure 5: *The correlator loss of a LFM pulse (T = 0.5 s and W = 200 Hz) in an isospeed channel with a rigid bottom. The contour plot shows four levels: CL = −17 dB (solid), −18 dB (dashed), −18.5 dB (dotted) and −19 dB (dashdot).*

PRN pulse – Rigid bottom

Figure 6: The correlator loss of a PRN pulse (T = 0.5 s and W = 200 Hz) in an isospeed channel with a rigid bottom. The contour plot shows four levels: CL = −18 dB (solid), −18.5 dB (dashed), −19 dB (dotted) and −19.5 dB (dashdot).
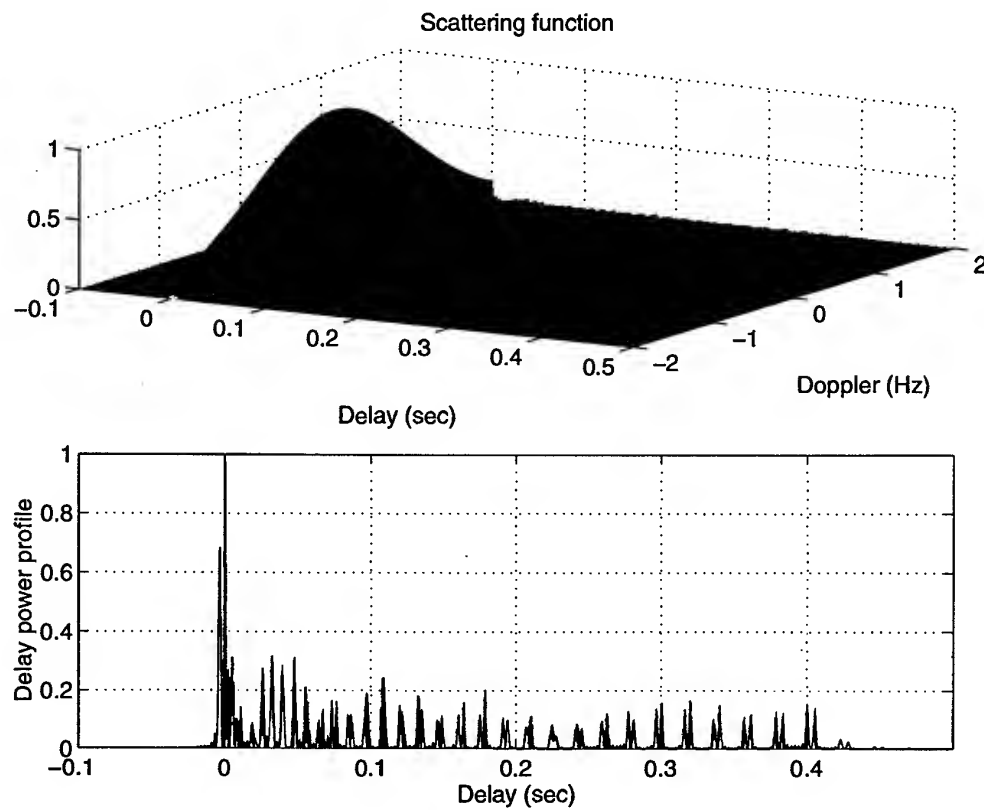
Scattering function

Delay (sec)

Doppler (Hz)

Figure 7: (a) Scattering function and (b) its Delay Power Profile for a target range, r = 10 km, and depth, z = 50 m. The channel is isospeed with a fluid bottom (c_b = 1600 m/s and ρ_b = 1500 kg/m³).
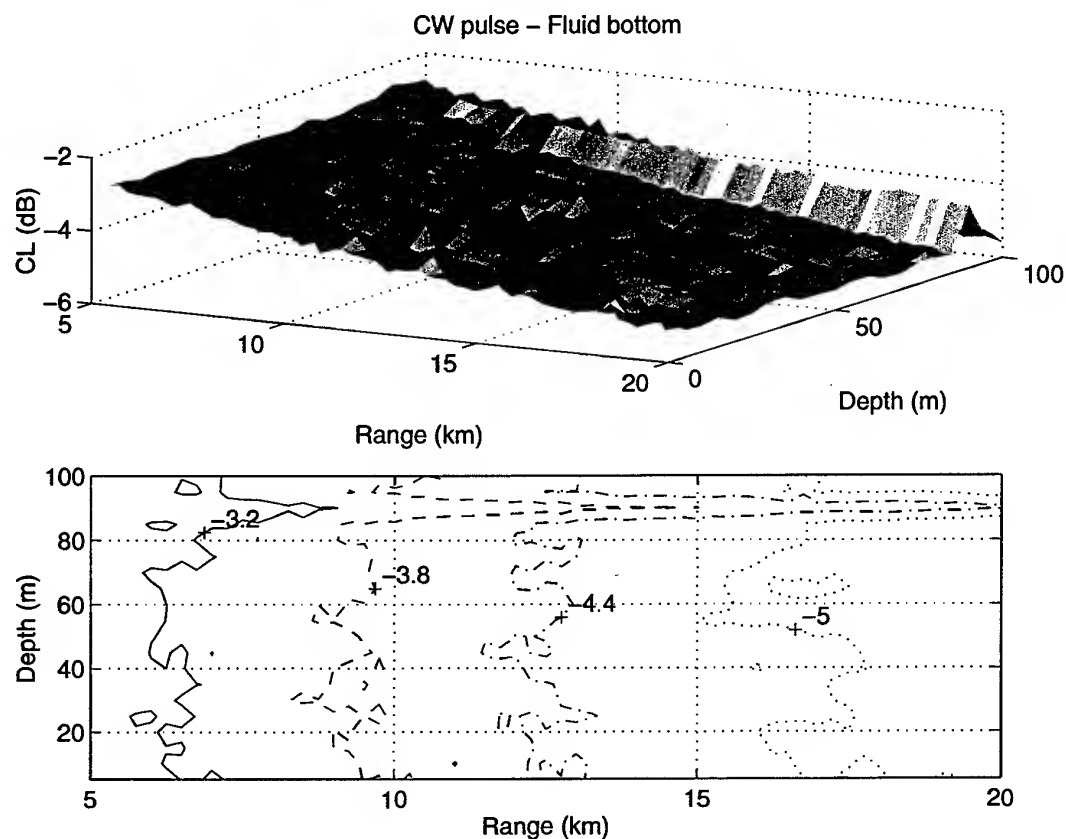
Figure 8: *The correlator loss of a CW pulse (T = 0.5 s) in an isospeed channel with a fluid bottom (c_b = 1600 m/s and ρ_b = 1500 kg/m³). The contour plot shows four levels: CL = −3.2 dB (solid), −3.8 dB (dashed), −4.4 dB (dashdot) and −5 dB (dotted).*
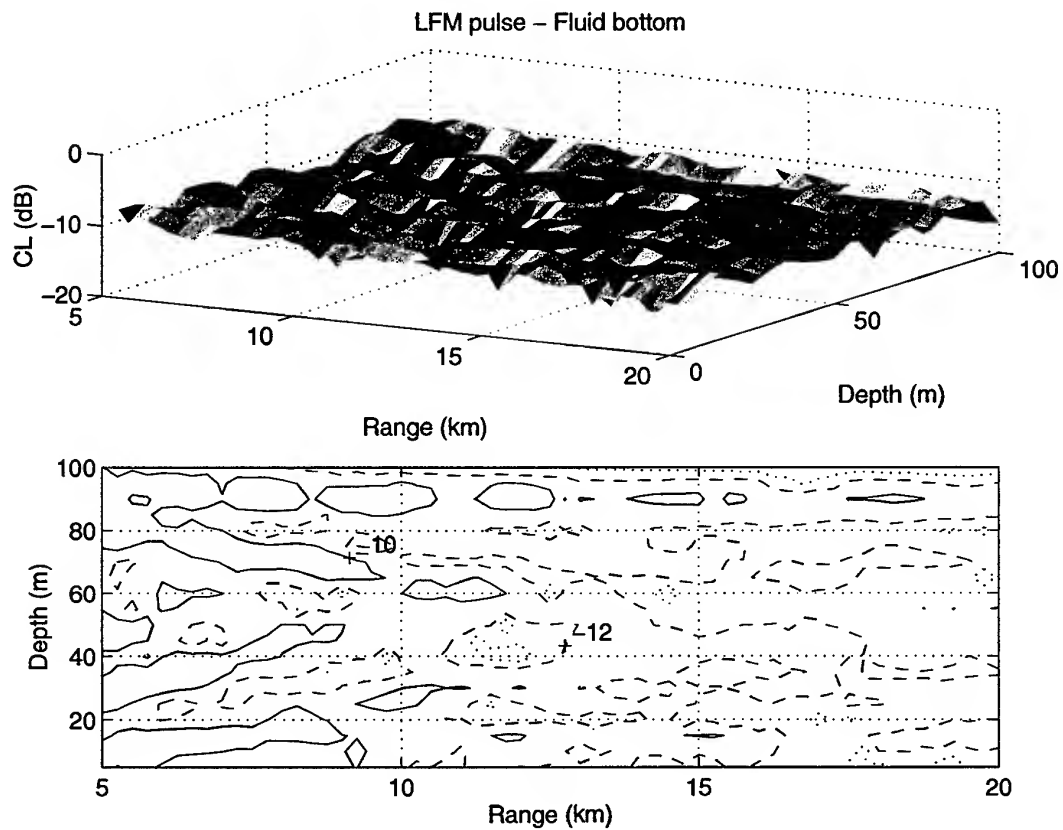
Figure 9: *The correlator loss of a LFM pulse (T = 0.5 s and W = 200 Hz) in an isospeed channel with a fluid bottom (c_b = 1600 m/s and ρ_b = 1500 kg/m³). The contour plot shows three levels: CL = −10 dB (solid), −12 dB (dashed), and −14 dB (dotted).*
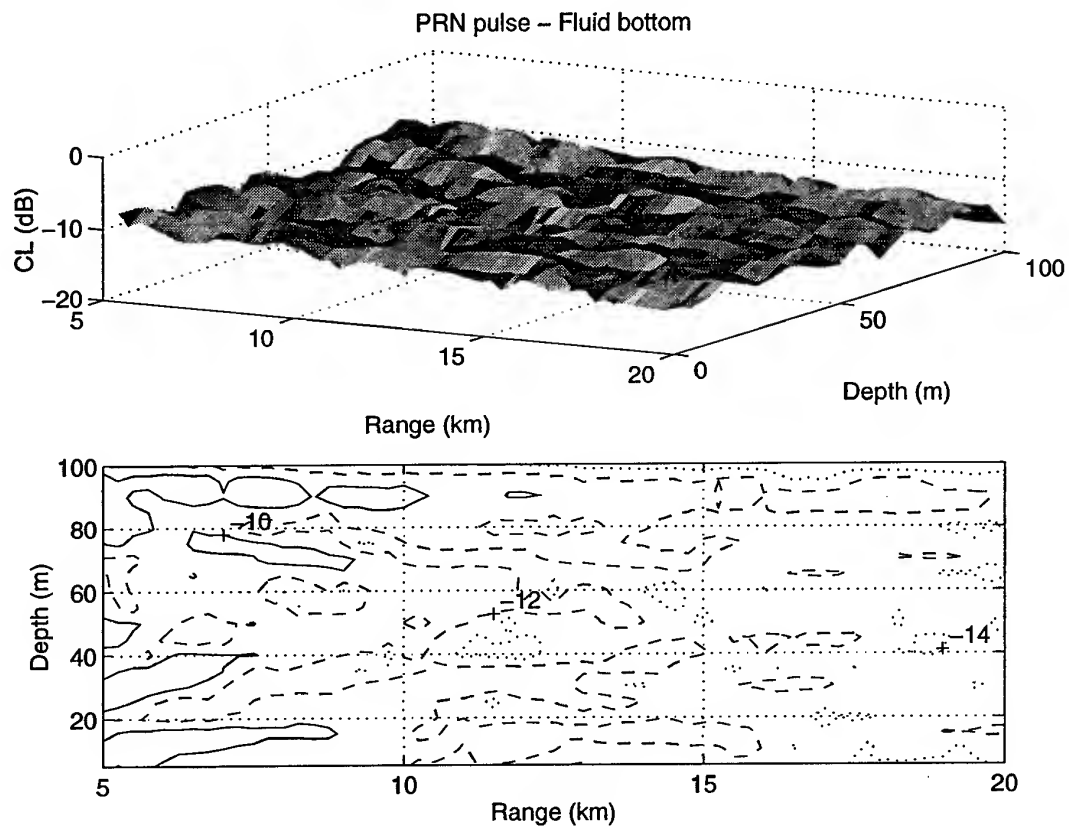
Figure 10: The correlator loss of a PRN pulse $(T = 0.5 \ s \ and \ W = 200 \ Hz)$ in an isospeed channel with a fluid bottom $(c_b = 1600 \ m/s \ and \ \rho_b = 1500 \ kg/m^3)$. The contour plot shows three levels: $CL = -10 \ dB \ (solid)$, $-12 \ dB \ (dashed)$, and $-14 \ dB \ (dotted)$.
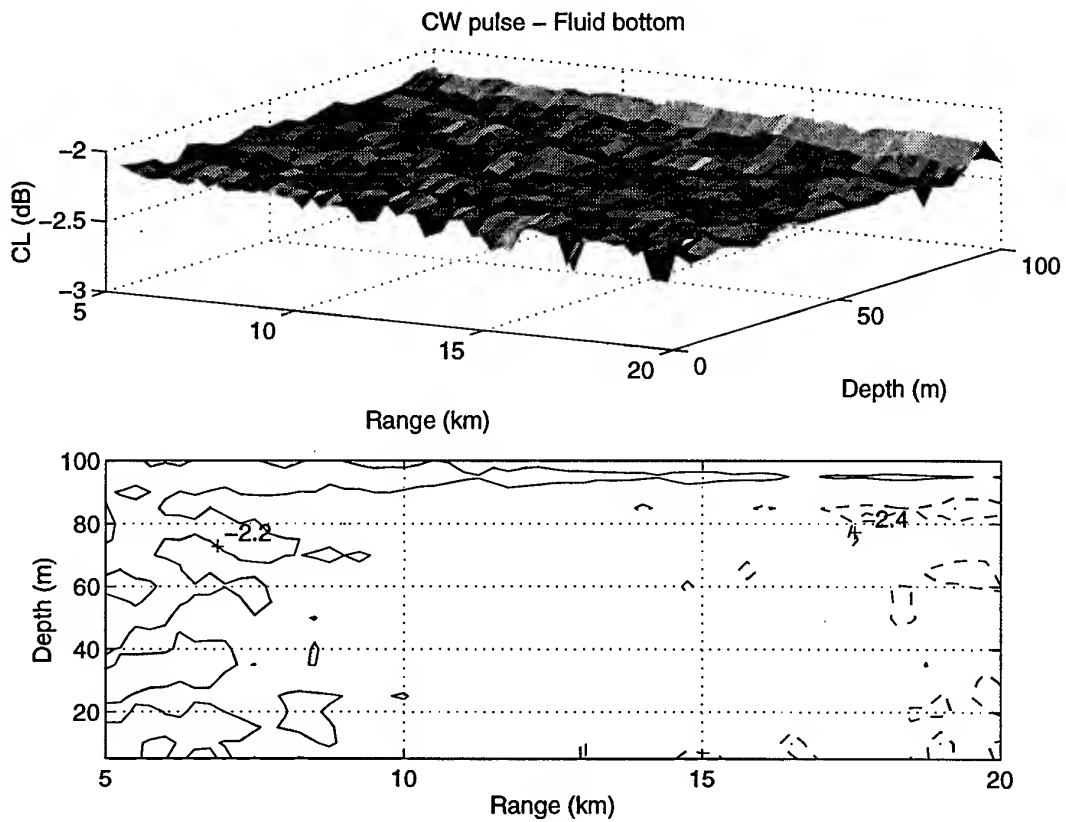
Figure 11: The correlator loss of a CW pulse (T = 0.5 s) in an isospeed channel with a fluid bottom (c_b = 1510 m/s and ρ_b = 1010 kg/m^3). The contour plot shows two levels: CL = −2.2 dB (solid) and −2.4 dB (dashed).

Figure 12: The correlator loss of a LFM pulse (T = 0.5 s and W = 200 Hz) in an isospeed channel with a fluid bottom (c_b = 1510 m/s and ρ_b = 1010 kg/m^3). The contour plot shows three levels: CL = −5 dB (solid), −7 dB (dashed), and −9 dB (dotted).
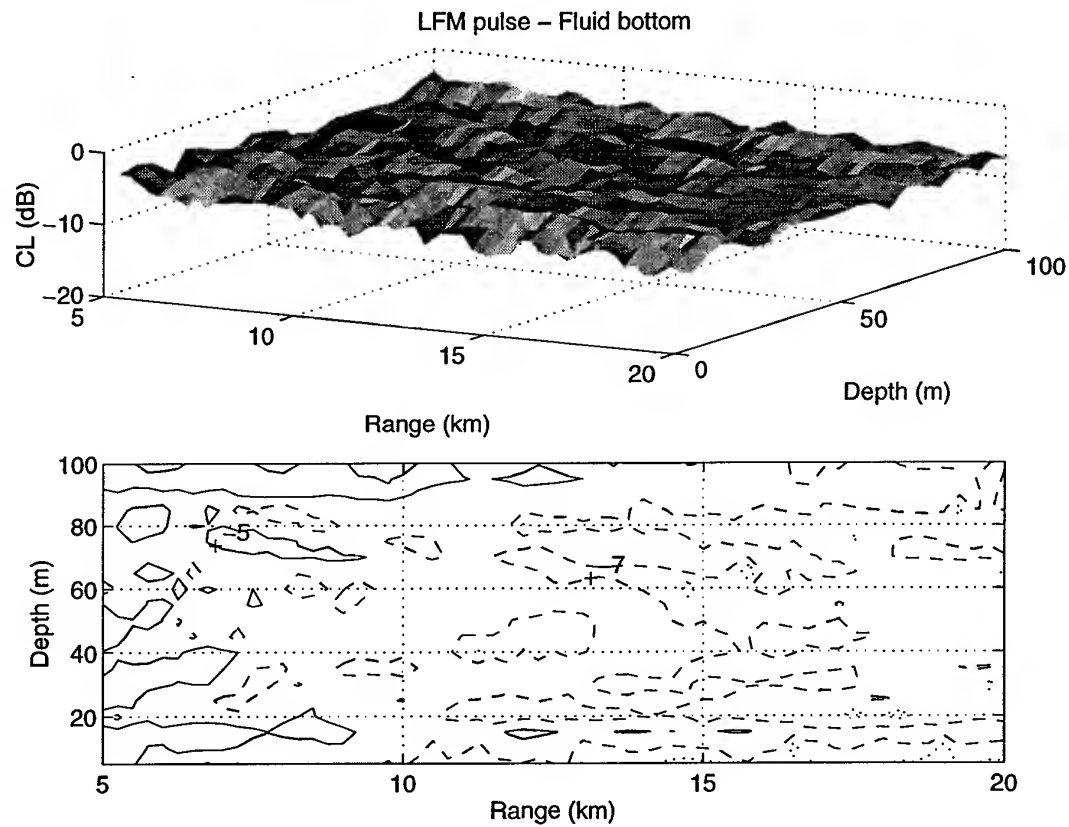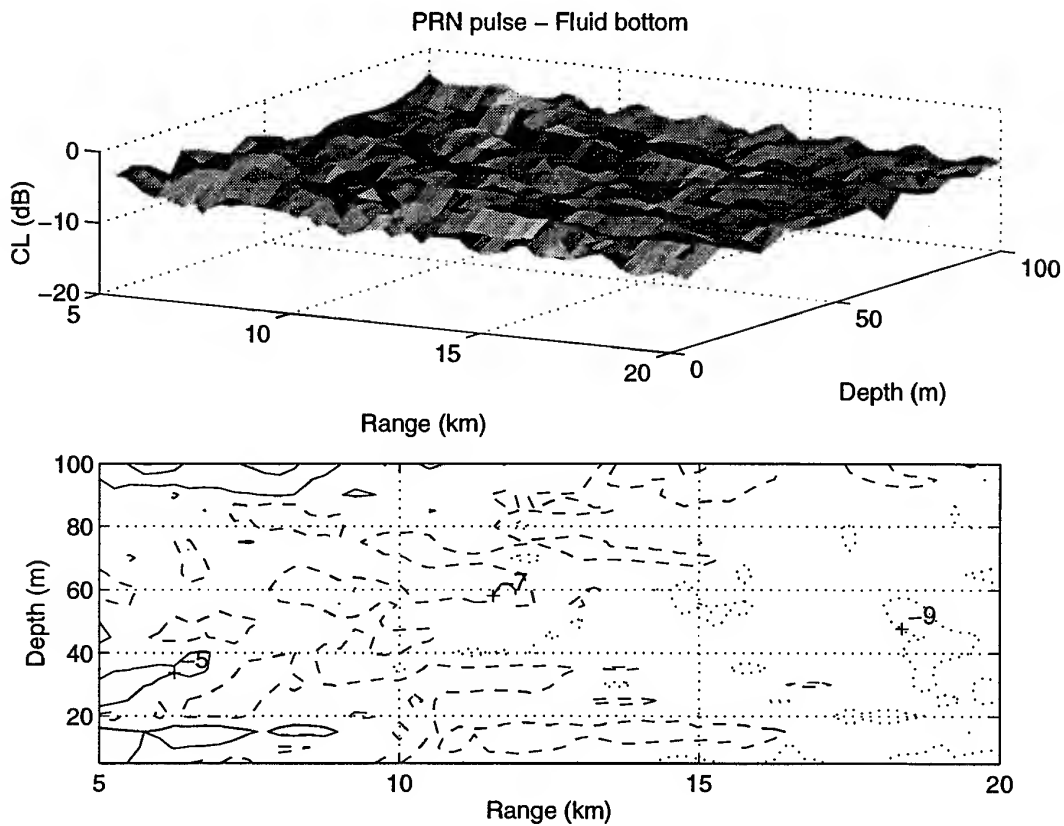
Figure 13: The correlator loss of a PRN pulse ($T = 0.5$ s and $W = 200$ Hz) in an isospeed channel with a fluid bottom ($c_b = 1510$ m/s and $\rho_b = 1010$ kg/m^3). The contour plot shows three levels: $CL = -5$ dB (solid), -7 dB (dashed), and -9 dB (dotted).

Scattering Function of Shallow Water Channels

H. Lew

AUSTRALIA

DEFENCE ORGANISATION

Task Sponsor
Director General Maritime Development
S&T Program
    Chief Defence Scientist

    FAS Science Policy   } shared copy

    AS Science Corporate Management
    Director General Science Policy Development
    Counsellor Defence Science, London (Doc Data Sheet)
    Counsellor Defence Science, Washington (Doc Data Sheet)
    Scientific Adviser to MRDC Thailand (Doc Data Sheet)
    Scientific Adviser Policy and Command
    Navy Scientific Adviser (Doc Data Sheet and distribution list only)
    Scientific Adviser - Army (Doc Data Sheet and distribution list only)
    Air Force Scientific Adviser
    Director Trials

    Aeronautical and Maritime Research Laboratory
    Director

    Chief of Maritime Operations Division
    G. Furnell, MOD Salisbury
    A. Jones, MOD Salisbury
    L. Kelly, MOD Salisbury
    A. Larsson, MOD Salisbury
    H. Lew, MOD Salisbury
    D. Liebing, MOD Salisbury
    J. Riley, MOD Salisbury
    D. Sweet, MOD Salisbury
    S. Taylor, MOD Salisbury
    J. Wang, MOD Salisbury

DSTO Library and Archives
    Library Fishermens Bend
    Library Maribyrnong
    Library Salisbury (2 copies)
    Australian Archives
    Library, MOD, Pyrmont
    Library, MOD, HMAS Stirling only
    *US Defense Technical Information Center, 2 copies
    *UK Defence Research Information Centre, 2 copies
    *Canada Defence Scientific Information Service, 1 copy
    *NZ Defence Information Centre, 1 copy
    National Library of Australia, 1 copy

Capability Development Division
 Director General Land Development (Doc Data Sheet only
 Director General C3I Development (Doc Data Sheet only)
 Director General Aerospace Development (Doc Data Sheet only)
 ASSTASS Project Director (Cmdr C. Donald, CP3-4-12)

Navy
 SO (Science), Director of Naval Warfare, Maritime Headquarters Annex,
  Garden Island, NSW 2000. (Doc Data Sheet only)

Army
 ABCA Office, G-1-34, Russell Offices, Canberra (4 copies)
 SO (Science), DJFHQ(L), MILPO Enoggera, Queensland 4051 (Doc Data Sheet only)
 NAPOC QWG Engineer NBCD c/- DENGRS-A, HQ Engineer Centre Liverpool Military Area,
  NSW 2174 (Doc Data Sheet only)

Intelligence Program
 DGSTA Defence Intelligence Organisation

Corporate Support Program
 OIC TRS, Defence Regional Library, Canberra

UNIVERSITIES AND COLLEGES
 Australian Defence Force Academy
  Library
  Head of Aerospace and Mechanical Engineering
 Serials Section (M list), Deakin University Library, Geelong, 3217
 Senior Librarian, Hargrave Library, Monash University
 Librarian, Flinders University

OTHER ORGANISATIONS
 NASA (Canberra)
 AGPS

OUTSIDE AUSTRALIA

ABSTRACTING AND INFORMATION ORGANISATIONS
 Library, Chemical Abstracts Reference Service
 Engineering Societies Library, US
 Materials Information, Cambridge Scientific Abstracts, US
 Documents Librarian, The Center for Research Libraries, US

INFORMATION EXCHANGE AGREEMENT PARTNERS
 Acquisitions Unit, Science Reference and Information Service, UK
 Library - Exchange Desk, National Institute of Standards and Technology, US

SPARES (5 copies)

Total number of copies: **58**

DEFENCE SCIENCE AND TECHNOLOGY ORGANISATION DOCUMENT CONTROL DATA		1. CAVEAT/PRIVACY MARKING	

2. TITLE	3. SECURITY CLASSIFICATION		
Scattering Function of Shallow Water Channels	Document (U) Title (U) Abstract (U)		

4. AUTHOR(S)	5. CORPORATE AUTHOR		
H. Lew	Aeronautical and Maritime Research Laboratory PO Box 4331, Melbourne Victoria Australia 3001		

6a. DSTO NUMBER DSTO–TR–0644	6b. AR NUMBER AR 010-484	6c. TYPE OF REPORT Technical Report	7. DOCUMENT DATE March 1998

8. FILE NUMBER M9505/13/68	9. TASK NUMBER NAV 96/083	10. SPONSOR GDMD	11. No OF PAGES 13	12. No OF REFS 8

13. DOWNGRADING / DELIMITING INSTRUCTIONS Not Applicable	14. RELEASE AUTHORITY Chief, Maritime Operations Division

15. SECONDARY RELEASE STATEMENT OF THIS DOCUMENT

Approved For Public Release

OVERSEAS ENQUIRIES OUTSIDE STATED LIMITATIONS SHOULD BE REFERRED THROUGH DOCUMENT EXCHANGE CENTRE, DIS NETWORK OFFICE, DEPT OF DEFENCE, CAMPBELL PARK OFFICES, CANBERRA, ACT 2600

16. DELIBERATE ANNOUNCEMENT

No Limitations

17. CITATION IN OTHER DOCUMENTS

No Limitations

18. DEFTEST DESCRIPTORS

Submarine Noise, Active Sonar, Noise Reduction, Acoustic Signatures, Detection

19. ABSTRACT

The time and frequency spreading of a shallow water acoustic channel can be characterized by its scattering function. In order to exploit some of the time delay regularities in the acoustic channel, the scattering function is calculated using a Pekeris waveguide model. The correlator loss, which is a measure of the amount of signal spreading caused by the channel, is calculated as a function of range and depth for three well known classes of signals used in active sonar.